Volume 45 | Number 20 | 28 May 2016 | Pages 8303–8660

Dalton Transactions

An international journal of inorganic chemistry

www.rsc.org/dalton

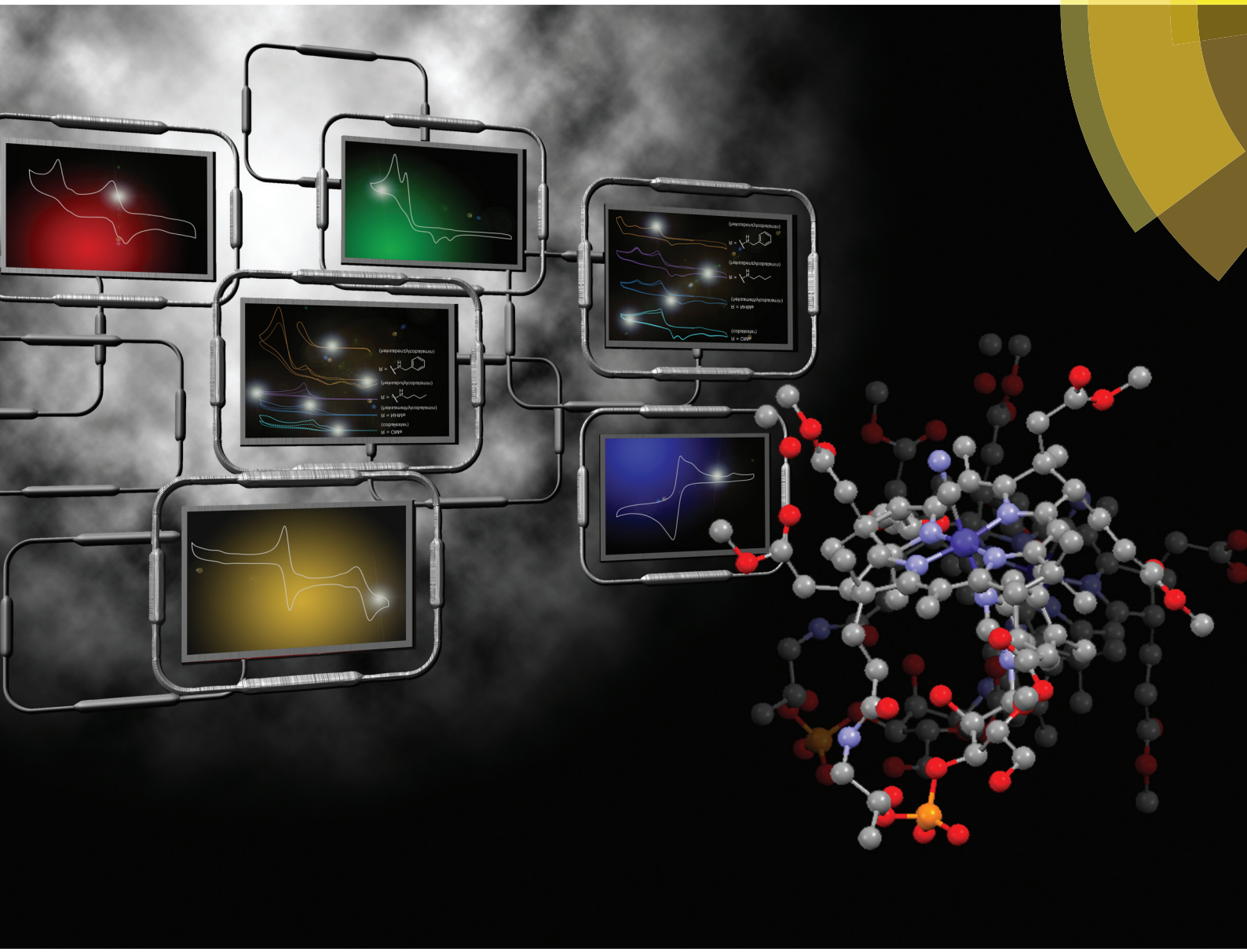

ISSN 1477-9226

ROYAL SOCIETY OF CHEMISTRY

PAPER

H. Shimakoshi, D. Gryko, Y. Hisaeda *et al.*

Electrochemistry and catalytic properties of amphiphilic vitamin B_{12} derivatives in nonaqueous media

175 YEARS

Dalton Transactions

PAPER

View Article Online
View Journal | View Issue

CrossMark click for updates

Cite this: *Dalton Trans.*, 2016, **45**, 8340

Electrochemistry and catalytic properties of amphiphilic vitamin B_{12} derivatives in nonaqueous media†

M. Giedyk,[a] H. Shimakoshi,*[b] K. Goliszewska,[a] D. Gryko*[a] and Y. Hisaeda*[b]

Received 25th January 2016,
Accepted 29th February 2016

DOI: 10.1039/c6dt00355a

www.rsc.org/dalton

The reduction pathway of cobalester (CN)Cble, an amphiphilic vitamin B_{12} derivative, was investigated in organic solvents under electrochemical conditions and compared with mono- and dicyanocobyrinates. The redox characteristics were determined using cyclic voltammetry and spectroelectrochemical methods. The presence of a nucleotide moiety in B_{12}-derivative impedes the *in situ* formation of dicyano-species thus facilitating the (CN)Co(III) to Co(I) reduction. The (CN)Cble shows stepwise reduction to Co(I) *via* (CN)Co(II). The reduction of (CN)Co(II)/Co(I) was found to depend on cyanide-solvent exchange equilibrium with weakly coordinating solvents and bulky peripheral chains promoting intact (CN)Co(II) species existence. The studied complexes were also utilized as catalysts in bulk electrolysis of benzyl bromide affording bibenzyl in very good yield.

Introduction

Vitamin B_{12} (cyanocobalamin **1**) is a highly functionalised organometalic complex comprising a corrin ring with the central cobalt cation and peripheral amide chains as shown in Fig. 1.[1,2] As a cofactor for B_{12}-dependent enzymes it plays an important role in the normal functioning of mammalian organisms.[3–5] Inspired by nature, scientists successfully employed cyanocobalamin (**1**) and its derivatives as catalysts in organic synthesis, due to their ability to form and selectively cleave Co–C bonds.[6–9] The scope of B_{12}-catalyzed reactions is continuously expanding, now including such processes as dehalogenation, addition to double bonds, ring expansion, C–H functionalization *etc*.

The catalytic properties of vitamin B_{12} derivatives rely on redox chemistry of the central cobalt cation with the reduction of Co(III) to active Co(II) or Co(I) forms being critical.[10] Therefore, the understanding of their electrochemistry becomes an essential element for the rational design and successful application of B_{12}-catalyzed reactions.

Even though the natural, nontoxic, and stable cyanocobalamin (**1**) may appear as an ideal catalyst, it suffers from low solubility in synthetically useful organic solvents such as DCM, MeCN, THF *etc*. Hence, modification of its structure is commonly performed giving access to more lipophilic derivatives.[11] For example, the synthesis and utilization of heptamethyl cobyrinates (*e.g.* monocyanocobyrinate **3**) have been well established.[12–17] An alternative approach was recently reported by Gryko *et al.* who synthesized cobalester ((CN)Cble, **2**) – a derivative possessing six ester groups on the periphery of the corrin ring with the nucleotide fragment intact that displays good solubility both in aqueous and in organic media.[18] A direct comparison of derivatives with and without the nucleotide loop became thereby possible.

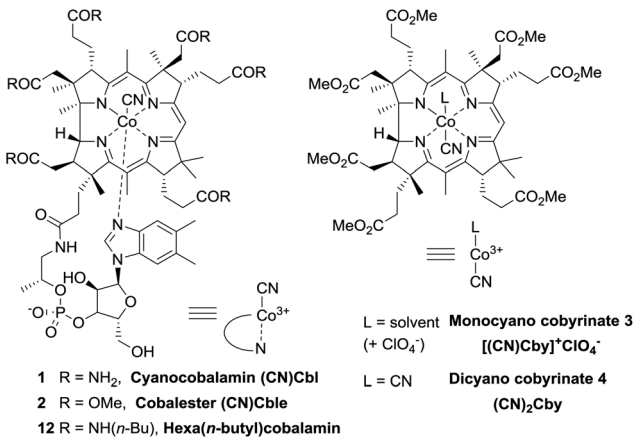

Fig. 1 Structures and abbreviations of vitamin B_{12} derivatives.

[a]*Institute of Organic Chemistry Polish Academy of Sciences, Kasprzaka 44/52, 01-224 Warsaw, Poland. E-mail: dorota.gryko@icho.edu.pl; http://ww2.icho.edu.pl/gryko_group*

[b]*Department of Chemistry and Biochemistry, Graduate School of Engineering, Kyushu University, Fukuoka, 819-0395, Japan. E-mail: shimakoshi@mail.cstm.kyushu-u.ac.jp, yhisatcm@mail.cstm.kyushu-u.ac.jp*

†Electronic supplementary information (ESI) available: Details of mechanistic studies, spectroscopic data of (CN)Cble (**2**), $[(CN)Cby]^+ClO_4^-$ (**3**), and hexa(*n*-butyl)cobalamin (**12**). See DOI: 10.1039/c6dt00355a

Whereas the redox characteristics of cobyrinate derivatives in organic solvents have been extensively studied by Murakami and Hisaeda,[19–21] no suitable data are available for cobalester (**2**). We wondered whether the nucleotide fragment influences the redox behavior and catalytic activity of cobalamin derivatives in organic solvents, preferred in organic synthesis.

Herein, we present the redox characteristics of cobalester (**2**) with regard to factors influencing the reduction of Co(III) to catalytically active Co(II) and Co(I) species and demonstrate its application as a catalyst in potential-controlled electrolysis of benzyl bromide.

Results and discussion

Cyclic voltammetry of vitamin B_{12} derivatives in organic solvents

In order to understand the influence of the nucleotide fragment on the redox behaviour of cobalesters (**2**) in organic solvents, a series of cyclic voltammograms was recorded. The use of a glassy carbon working electrode proved superior over Pt, allowing for the reproducible observation of spectra in a broad range of potentials with clear detection of reduction and oxidation peaks. The spectrum of cobalester (**2**) in MeCN displayed apparent one quasi-reversible reduction peak (E_{red}) at *ca.* −0.9 V *vs.* Ag–AgCl which corresponds to two-step reduction of complex **2**, leading to Co(I) species *via* (CN)Co(II) species (Fig. 2A). Such redox behaviour is in agreement with that observed by Lexa and Savéant for cyanocobalamin in water and DMSO,[22,23] but is distinctively different from heptamethyl cobyrinates **3** and **4** for which Co(III)/Co(II) and Co(II)/Co(I) redox couples are well separated (Fig. 2C and D). This indicates an efficient formation of Co(I) species of cobalester (**2**) at less negative potentials compared to cobyrinate derivatives having the cyanide ligand.

Subsequently, we evaluated if and how the presence of an excess of the cyanide anion influences the redox properties of cobalester (**2**). A series of measurements were performed, proving that the two-electron reduction peak shifts towards the cathodic side (E_{red} = −1.2 V *vs.* Ag–AgCl) with the total current remaining the same (Fig. 2B). Supposedly, this was caused by the formation of the base-off $(CN)_2$Co(III) form with an electron rich cobalt centre which is more difficult to reduce. A similar observation has already been described for cyanocobalamin (**1**).[22]

Electronic spectra of vitamin B_{12} derivatives in organic solvents

Subsequently, cyanocobalester (**2**) was examined using controlled-potential electronic spectroscopy. The spectrum recorded after 15 min of electrolysis at −1.0 V *vs.* Ag–AgCl revealed the presence of expected Co(I) species with the absorption maximum at 390 nm, which was accompanied by a by-product exhibiting maximum absorption at 370 and 580 nm wavelengths that are characteristic for $(CN)_2$Co(III) species (Fig. 3A).

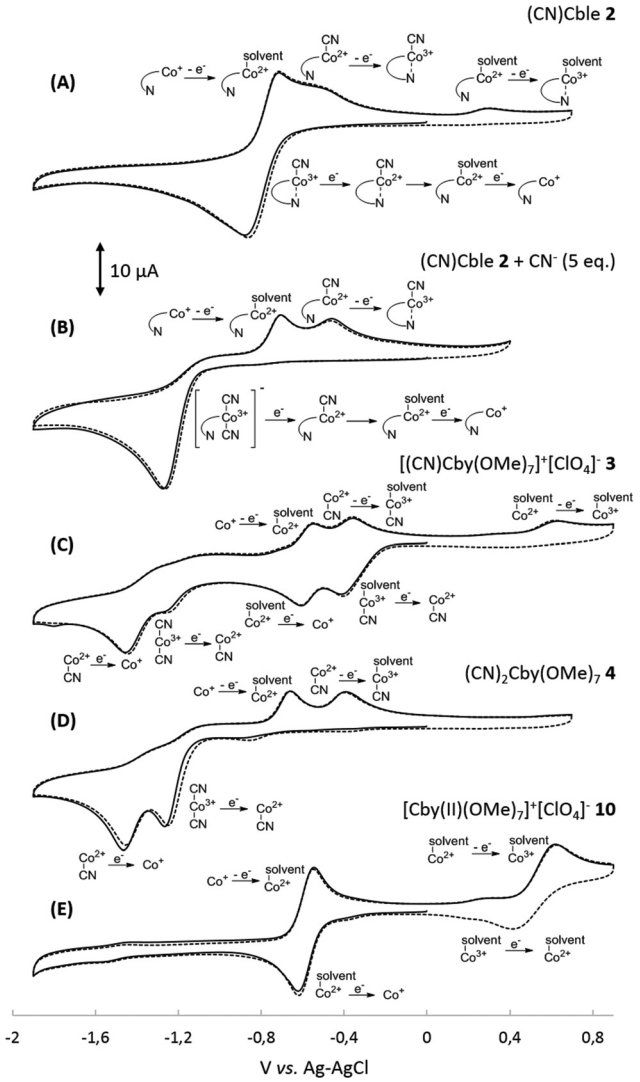

Fig. 2 Cyclic voltammograms of 1.0 mM MeCN solutions of: (A) cyanocobalester (**2**), (B) cyanocobalester (**2**) with addition of $Bu_4N^+CN^-$ (5 eq.), (C) monocyanocobyrinate (**3**), (D) dicyanocobyrinate, and (E) cobalt(II) cobyrinate (**4**). All solutions contained 0.1 M $Bu_4N^+ClO_4^-$ and measurements were carried out at room temperature under a nitrogen atmosphere using the GC working electrode and Pt counter electrode; sweep rate: 0.1 V s^{-1}.

The absorption bands did not disappear upon prolonging the time of electrolysis, but once the potential was lowered to −1.4 V *vs.* Ag–AgCl, a mixture quantitatively transformed into a final Co(I) form. Such a behaviour proves the *in situ* formation of the $(CN)_2$Co(III) complex from cyanocobalester (**2**) and CN^- released during its electrolysis (Fig. 3A). The working hypothesis was confirmed by superimposing the spectrum of the mixture with the one recorded for the solution of $[(CN)_2Cble]^-$ (prepared by mixing cyanocobalester with 5 eq. of $Bu_4N^+CN^-$) (see the ESI†). The formation of the cobalt(III) dicyano-complex was also observed when monocyanocobyrinate **3** was subjected to electrolysis at −1.0 V *vs.* Ag–AgCl (Fig. 3B). In this case the presence of the $(CN)_2$Co(III) complex was even more

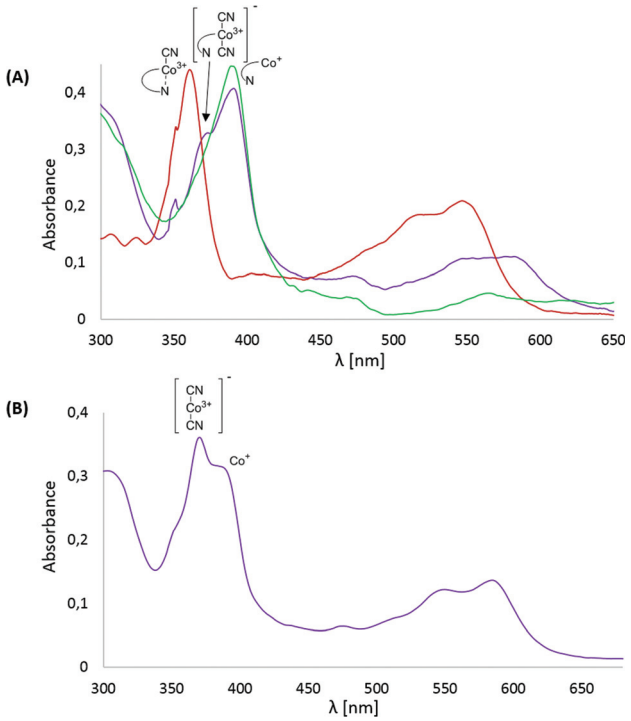

Fig. 3 Electronic spectra of 0.33 mM solution in MeCN of: (A) (CN)Cble (**2**) (red), (CN)Cble (**2**) subjected to 15 min electrolysis at −1.0 V *vs.* Ag–AgCl (purple) and fully reduced (CN)Cble (**2**) (green, 15 min electrolysis at −1.4 V *vs.* Ag–AgCl); (B) $[(CN)Cby]^{+}ClO_4^{-}$ (**3**) subjected to 15 min reduction at −1.0 V *vs.* Ag–AgCl. All solutions contained 0.1 M $Bu_4N^{+}ClO_4^{-}$ and measurements were carried out at room temperature under a nitrogen atmosphere using the carbon grid ITO working electrode and Pt counter electrode.

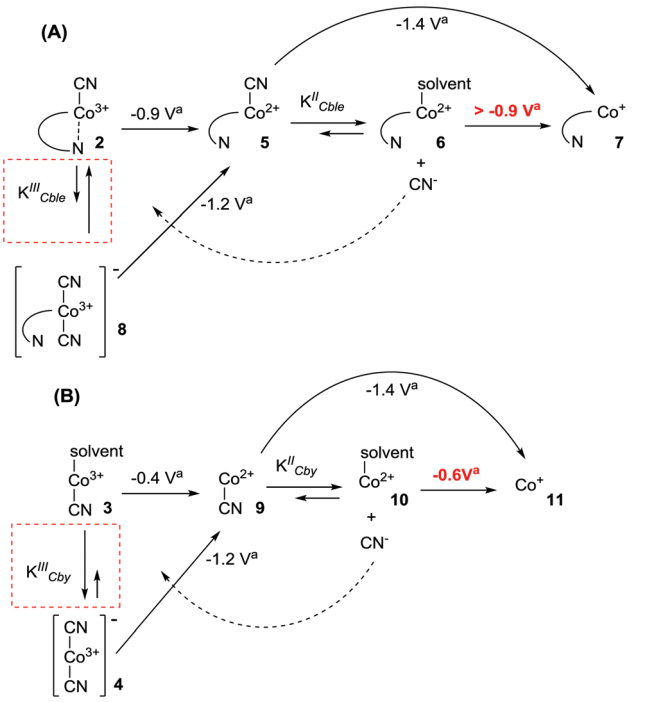

Scheme 1 Proposed mechanism for the reduction of: (A) cobalester (**2**) and (B) monocyanocobyrinate (**3**). [a]*vs.* Ag–AgCl.

pronounced as it was dominating over Co(I) species. The difference in the amount of $(CN)_2Co(III)$ formation was also detectable by cyclic voltammetry. No formation of dicyanocobalester was observed in **2** (Fig. 2A) within the time scale of the measurement, while the spectrum of cobyrinate **3** having no nucleotide fragment showed a reduction peak at *ca.* −1.2 V *vs.* Ag–AgCl (Fig. 2C), revealing the presence of $(CN)_2Co(III)$ complex **4**.

Mechanistic aspects of the reduction process

The results presented above clearly demonstrate the existence of $(CN)Co(III)/(CN)_2Co(III)$ equilibrium during the reduction of compounds **2** and **3** (Scheme 1), with the cyanide binding equilibrium constant for monocyano cobyrinate **3** much higher than the one for cobalester **2** ($K^{III}_{Cble} < K^{III}_{Cby}$). This stays in agreement with reports by Zelder, who studied cyanide complexation by cobalamin and cobinamide derivatives.[24,25] After identification of dicyano-compounds **4** and **8** as important intermediates in the reduction pathways, the attention was focused on the mechanism of the Co(I) species formation. Murakami *et al.* proposed (CN)Co(II) complex **9** as an intermediate formed in the first step upon monocyano cobyrinate **3** reduction in DMF.[20] This in turn supposedly undergoes further reduction to Co(I) species **11** at *ca.* −1.4 V *vs.* Ag–AgCl. While this is consistent with our observations for monocyano cobyrinate **3** in MeCN, the spectrum of cobalester (**2**) did not reveal such a negatively located signal in CV. Therefore, an exchange of the cyanide anion coordinating (CN)Co(II) **5** for a solvent molecule was considered (Scheme 1). In the first step of the reduction (at *ca.* −0.9 V and −0.4 V *vs.* Ag–AgCl for compounds **2** and **3** respectively), (CN)Co(II) species **5** and **9** were formed. Additionally to direct reduction at −1.4 V *vs.* Ag–AgCl, they could also undergo axial ligand exchange to yield (solvent)Co(II) complexes **6** and **10**, which are readily reduced at more positive potentials. This stays in contrast to what was proposed for cyanocobalamin (**1**) in protic solvents, where no (CN)Co(II) intermediate was considered in the absence of purposely added cyanide.[23] Furthermore, as it is generally accepted that the benzimidazole moiety in vitamin B_{12} possesses stronger electron donating abilities than MeCN, the mechanism involving base-on Co(II) form **7** would require more negative potentials. On the other hand, the equilibrium of Co(II)base-on/Co(II)base-off should not favour the base-on form in MeCN as it does in water. This allowed us to exclude the pathway involving the base-on Co(II) complex as less favoured.

To further confirm the existence of (CN)Co(II) intermediate **5** and a key role of axial ligand exchange in the generation of Co(I) species **7**, the reaction environment was modified in the following manner (Fig. 4). Firstly, the cyclic voltammogram was recorded using THF as a solvent. In contrast to the experiment in MeCN, a second reduction peak appeared at

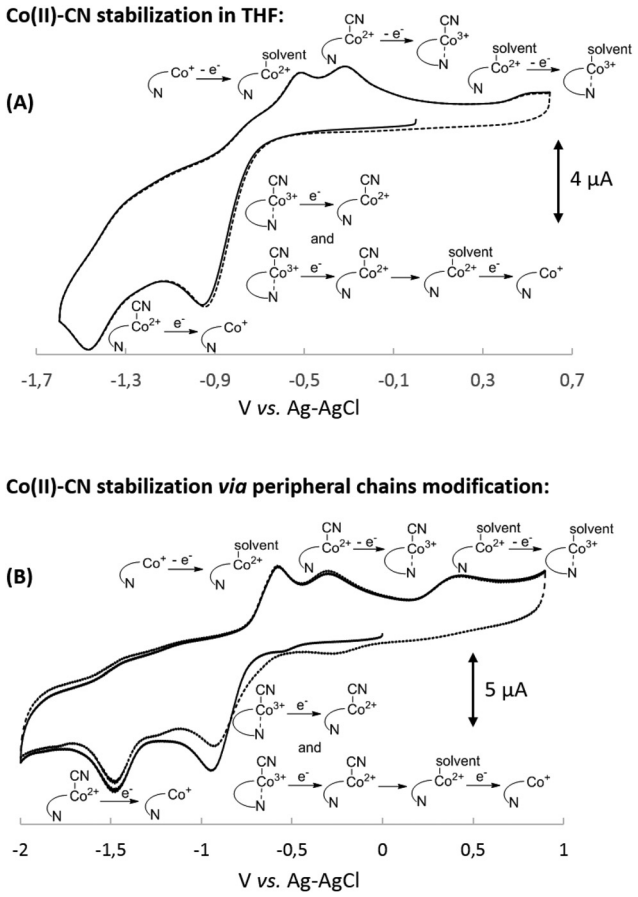

Fig. 4 Cyclic voltammograms of 1.0 mM solutions of: (A) cyanocobalester (**2**) in THF and (B) hexabutylcobalamin (**12**) in MeCN. All solutions contained 0.1 M $Bu_4N^+ClO_4^-$ and measurements were carried out at room temperature under a nitrogen atmosphere using the GC working electrode and Pt counter electrode; sweep rate: 0.1 V s^{-1}.

ca. −1.4 V *vs.* Ag–AgCl, indicating the direct reduction of cyano-form **5** to Co(I) complex **7**. Such a behavior is consistent with our mechanistic hypothesis, as weaker coordination abilities (compared to MeCN) towards transition metals result in a lower K^{II}_{Cble} value and afford stabilization of (CN)Co(II) complex **5** under the experimental conditions (Scheme 2). Secondly, hexabutylcobalamin (**12**) was synthesized by $Bu_4N^+CN^-$-catalyzed aminolysis of cobalester (**2**) and examined using cyclic voltammetry. Due to changes at the periphery of the corrin ring, we expected cyanide ligand exchange to be altered. Indeed, a peak assigned to direct (CN)Co(II)/Co(I) reduction was observed (Fig. 4B), thus supporting our proposed mechanism in Scheme 1.

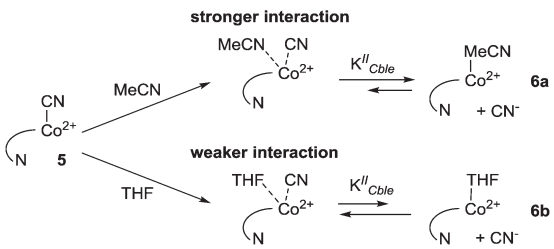

Scheme 2 Interactions of solvent molecules with (CN)Co(II) complex **5**.

Redox behaviour of amphiphilic vitamin B_{12} in the presence of benzyl bromide

With our quest to understand the catalytic activity of vitamin B_{12} derivatives in a nonaqueous environment, we examined the redox behaviour of cobalester (**2**) in the presence of benzyl bromide. We have previously reported that cobalester (**2**) catalyzes dimerization of various benzyl bromides in the microwave-assisted reaction yielding substituted bibenzyl derivatives in high yields.[18] A control measurement of benzyl bromide solution revealed a direct reduction peak at negative potential (E_{red} = −1.9 V *vs.* Ag–AgCl) (Fig. 5A). The addition of cobalester (**2**) (10 mol%) shifted the signal towards the anodic side by *ca.* 0.5 V marking a catalytic current (Fig. 5B). Moreover, when the scan was reversed at −0.95 V *vs.* Ag–AgCl, no reversible wave was observed (see the ESI†). This implies that once Co(I) species **7** is generated, it rapidly reacts with the electrophile forming complex **13** with the cobalt–carbon bond. The presence of a plateau between −0.9 and −1.0 V *vs.* Ag–AgCl indicated the stability of complex **13** in this range of the spectrum. Further negative sweeping of the potential might cause reduction of complex **13** to anion radical **14** that decomposed forming a benzyl radical and regenerating the active form of catalyst **7** (Scheme 3).

Controlled-potential electrolysis of benzyl bromide

The controlled-potential electrolysis of benzyl bromide in the presence of (CN)Cble (**2**) gave bibenzyl (Table 1). ESI MS analysis of the reaction mixture revealed the presence of Co-benzyl intermediate **13** (see the ESI†).

The use of carbon felt as a working electrode proved superior over Pt, which was consistent with the conditions of

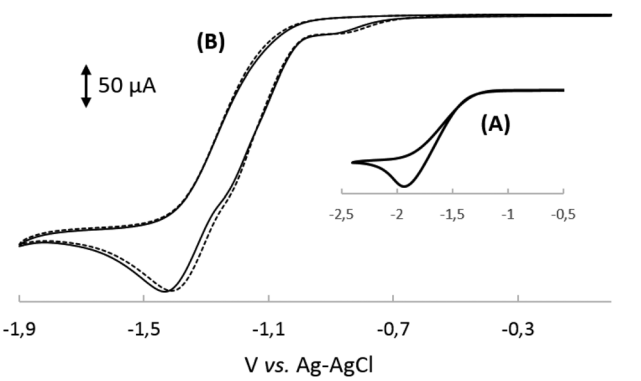

Fig. 5 Cyclic voltammograms of MeCN solutions of: (A) benzyl bromide (10 mM) and (B) cyanocobalester **2** (1.0 mM) in the presence of BnBr (10 mM). All solutions contained 0.1 M $Bu_4N^+ClO_4^-$ and measurements were carried out at room temperature under a nitrogen atmosphere using the GC working electrode and Pt counter electrode; sweep rate: 0.1 V s^{-1}.

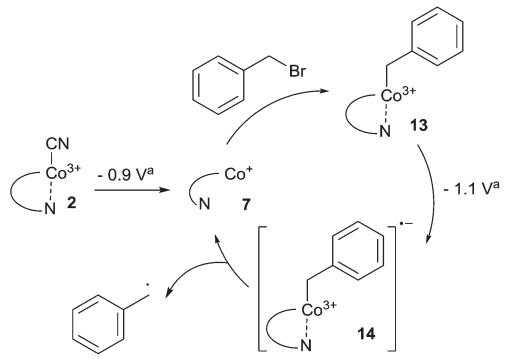

Scheme 3 Cobalester-catalyzed generation of the benzyl radical *via* intermediate Co–C species **13** and **14**. [a] *vs.* Ag–AgCl.

Table 1 Optimisation of the catalytic reaction[a]

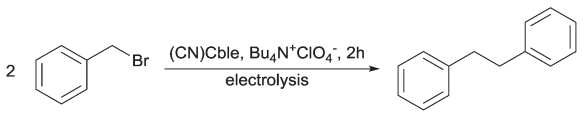

Entry	Working electrode	Potential[b] [V]	Yield[c] [%]
1	Pt	−1.1	69
2	Carbon-felt	−1.1	76
3[d]	Carbon-felt	−1.1	13
4[e]	Carbon-felt	−1.1	71
5	Carbon-felt	−1.0	67
6[f]	Carbon-felt	−1.1	13

[a] Controlled-potential electrolyses were carried out in MeCN under a N_2 atmosphere at rt using a divided cell system with the Zn counter-electrode. Initial concentration in the working-electrode compartment: BnBr: 0.25 M, (CN)Cble **2**: 1.25 mM, $Bu_4N^+ClO_4^-$: 0.2 M. [b] *vs.* Ag–AgCl. [c] The quantity of the product is the average of at least two repeated experiments from the GC-MS results. [d] Reaction performed in THF. [e] 0.125 M solution of benzyl bromide was used. [f] No catalyst.

cyclic voltammetry measurements (compare entries 1 and 2). Among potentials examined, −1.1 V *vs.* Ag–AgCl was optimal giving the yield of 76% (entry 2). As expected, the use of THF as a solvent (entry 3) led to a dramatic decrease in the yield, due to impeded generation of active Co(I) species **7**. Lowering the concentration of the starting material only slightly affected the yield (entry 4). As for the applied potential, −1.0 V *vs.* Ag–AgCl still allowed for an efficient reaction to occur (entry 5), however, no further decrease was possible (data not shown). The background reaction without the addition of the catalyst gave the desired product in low yield (entry 6).

Next we examined cobyrinate-derived complexes **3** and **4** as catalysts in bulk electrolysis (Table 2). Surprisingly, changing the catalyst to $[(CN)Cby]^+ClO_4^-$ (**3**) did not affect the reaction outcome (compare entries 1 and 2). This stays in contrast to the efficiency of Co(I) form generation which was proven to be higher for catalyst **2**. Furthermore, the use of $(CN)_2Cby$ (**4**) afforded the product in comparable yield, suggesting a shift in Co(I) formation equilibria which is caused by the irreversible reaction of Co(I) species **7** with benzyl bromide. Moreover, once the active Co(I) complex is formed, it recovers in the catalytic cycle, masking initial differences.

Table 2 Comparison of B_{12} derivatives as catalysts[a]

Entry	Catalyst	Conversion[b] [%]	Yield[b] [%]
1	(CN)Cble (**2**)	95	76
2	$[(CN)Cby]^+ClO_4^-$ (**3**)	88	76
3	$(CN)_2Cby$ (**4**)	86	64

[a] Controlled-potential electrolyses were carried out at −1.1 V *vs.* Ag–AgCl in MeCN under a N_2 atmosphere at rt using a divided cell system with the carbon-felt working electrode and Zn counter-electrode. Initial concentration in the working-electrode compartment: BnBr: 0.25 M, catalyst: 1.25 mM, $Bu_4N^+ClO_4^-$: 0.2 M. [b] The quantity of the product is the average of at least two repeated experiments from the GC-MS results.

Conclusions

In conclusions, for the first time, the reduction pathway for cobalester (**2**) was determined in aprotic solvents and compared with mono- and dicyanocobyrinates **3** and **4**. The reaction mechanism involves axial cyanide exchange which depends on the coordination abilities of a solvent, as well as the steric hindrance around the cobalt centre. Furthermore, it was found that the reduction process is influenced by the affinity of the cobalt cation to cyanide, which results in the formation of stable dicyano-species **4** and **8**. The latter feature, however, does not determine the outcome of Co(I)-catalyzed bulk electrolysis of benzyl bromide, as the irreversible formation of the Co-benzyl complex facilitates the reduction process.

Our findings provide a new insight into B_{12} derivatives redox chemistry in an organic, aprotic environment. We expect that the understanding of factors that influence the generation of active Co(I) will soon result in the development of new B_{12}-catalyzed organic reactions.

Experimental

Materials

All solvents and chemicals were of reagent grade and used without further purification. Dry MeCN, THF and *N*,*N*-dimethylformamide (DMF) were purchased from Wako Chemicals. Tetra(*n*-butyl)ammonium perchlorate (n-$Bu_4N^+ClO_4^-$) was purchased from Sigma Aldrich. Cyanocobalester **2**, monocyanocobyrinate **3** and dicyanocobyrinate **4** were synthesized according to reported procedures.[12,18,26]

General analysis and measurements

The electronic absorption spectra were recorded using a Hitachi U-3000 spectrophotometer and a 10 mm cell.

The cyclic voltammograms were obtained using a BAS ALS-630C electrochemical analyzer. The gas chromatography-

mass spectra (GC-MS) were obtained using a Shimadzu GCMS-QP5050 equipped with a J&W Scientific DB-1 column (length: 30 m; ID: 0.25 mm, film: 0.25 μm) and helium as the carrier gas. For the measurement, the injector and detector temperatures were 250 °C, the oven temperature was initially held at 40 °C for 4 min, and then increased to 240 °C at a rate of 10 °C min^{-1}. The ESI-MS was measured by using a JMS-T100LC AccuTOF from JEOL.

The spectroelectrochemical measurements for **2** and **3** were carried out in MeCN containing of 0.1 M *n*-$Bu_4N^+ClO_4^-$ under N_2 with a BAS SEC2000 spectrometer equipped with carbon-grid ITO glass as a working electrode, a Pt wire as an counter electrode, and an Ag/AgCl electrode (3 M aq. NaCl) as the reference.

Cyclic voltammetry

A cylindrical three-electrode cell that was used was equipped with a glassy carbon working electrode, a 25 mm platinum wire as the counter electrode and an Ag/AgCl (3.0 M NaCl) electrode as the reference electrode. The scan rate for a typical experiment was 100 mV s^{-1}. The dry solution of the vitamin B_{12} derivatives (1.0×10^{-3} M) and *n*-$Bu_4N^+ClO_4^-$ (1.0×10^{-1} M) was deaerated by N_2 gas bubbling before the measurements, and the cyclic voltammetry was carried out under a N_2 gas atmosphere at room temperature. The $E_{1/2}$ value of the ferrocene–ferrocenium (Fc/Fc^+) was 0.56 V *vs.* Ag/AgCl with this setup.

Catalytic benzyl bromide dimerization reaction under electrochemical conditions

Controlled-potential electrolyses were carried out in dry MeCN at −1.1 V *vs.* Ag/AgCl under a N_2 atmosphere in a divided electrolysis cell separated by a polypropylene membrane. The cathodic compartment was equipped with a Pt mesh or a carbon felt working electrode, an Ag/AgCl (3 M aq. NaCl) reference electrode and a stirring bar. The anodic compartment was equipped with a sacrificial Zn-plate electrode. The applied potential between the working and reference electrodes in the electrolysis was maintained constant with a Hokuto Denko HA BF-501A potentiostat, and the electrical quantity was also recorded on it. For a typical reaction, a MeCN solution of the vitamin B_{12} derivative (1.25×10^{-3} M), BnBr (2.5×10^{-1} M), *n*-$Bu_4N^+ClO_4^-$ (2.0×10^{-1} M) was deaerated by N_2 and subjected to electrolysis for 2 h at room temperature. Solutions from both compartments were then mixed together, passed through a silica pad and analyzed by GC-MS with biphenyl as the internal standard.

Synthesis of hexa(*n*-butyl)cobalamin (12)

A sealed pressure tube was charged with cyanocobalester (**2**, 15 mg, 1.0×10^{-2} mmol), $Bu_4N^+CN^-$ (17 mg, 6×10^{-2} mmol), dry MeOH (0.1 mL) *n*-butylamine (0.5 mL) and diethyl cyanophosphonate (30 μL, 2.0×10^{-1} mmol). The reaction mixture was stirred for 4 days at 55 °C. It was then diluted with CH_2Cl_2 and washed with 10% HCl, water and saturated $NaHCO_3$. The organic phase was dried over Na_2SO_4, filtered and concentrated *in vacuo*. The crude product was purified using reverse phase (C18) column chromatography (gradually from 50 to 75% MeOH in water) and subsequent chromatography on silica (gradually from 0 to 10% MeOH in toluene). Recrystallization from CH_2Cl_2/hexane gave a red solid (8 mg; 47%). HRMS ESI (*m*/*z*) calcd for $C_{87}H_{136}N_{14}O_{14}PCoNa_2$ $[M + 2Na]^{2+}$ 1736.92145, found 868.4607. UV/Vis (DMSO): λ_{max} (ε [l mol^{-1} cm^{-1}]) = 547 (8.65×10^3), 516 (7.59×10^3), 361 (2.56×10^4), 325 (8.75×10^3), 278 (1.67×10^4), 262 (1.66×10^4). Anal. calcd for $C_{87}H_{136}CoN_{14}O_{14}P + CH_2Cl_2$: C 59.48, H 7.83, N 11.04; found: C 59.50, H 7.83, N 10.40. ^{1}H NMR (500 MHz, CD_3OD): δ = 7.25 (s, 1H), 7.11 (s, 1H), 6.55 (s, 1H), 6.26 (d, J = 3.1 Hz, 1H), 6.03 (s, 1H), 4.70–4.63 (m, 1H), 4.57–4.51 (m, 1H), 4.37–4.28 (m, 1H), 4.19 (t, J = 3.5 Hz, 1H), 4.12–4.05 (m, 2H), 3.92–3.88 (m, 1H), 3.76–3.72 (m, 1H), 3.68 (d, J = 14.0 Hz, 1H), 3.63 (s, 1H), 3.49 (q, J = 5.2 Hz, 1H), 3.28–3.07 (m, 10H), 3.02–2.91 (m, 2H), 2.87–2.80 (m, 2H), 2.66–2.44 (m, 11H), 2.42–2.32 (m, 4H), 2.28–2.24 (m, 6H), 2.18–2.08 (m, 2H), 2.05–1.93 (m, 3H), 1.91–1.84 (m, 4H), 1.77–1.67 (m, 2H), 1.57–1.15 (m, 42H), 1.14–1.05 (m, 2H), 0.97–0.86 (m, 18H), 0.42 (s, 3H) ppm. ^{13}C NMR (125 MHz, CD_3OD): δ = 181.5, 180.2, 177.6, 175.6, 174.6, 174.4, 174.0, 173.6, 172.7, 172.5, 171.6, 167.2, 166.5, 143.4, 138.3, 135.4, 133.8, 131.5, 130.7, 117.9, 112.5, 109.0, 105.0, 95.6, 87.9, 86.5, 83.7, 76.2, 75.4, 73.7, 73.6, 71.5, 70.7, 62.7, 60.3, 57.8, 57.6, 55.0, 52.9, 46.85, 46.82, 45.2, 43.7, 40.6, 40.5, 40.4, 40.32, 40.28, 40.1, 36.9, 35.8, 33.6, 33.5, 33.0, 32.9, 32.7, 32.56, 32.55, 32.50, 32.4, 32.3, 30.7, 29.8, 27.7, 27.5, 23.7, 21.3, 21.24, 21.22, 21.17, 21.15, 21.1, 20.9, 20.43, 20.39, 20.3, 20.20, 20.17, 19.9, 17.6, 17.1, 16.3, 16.0, 14.10, 14.09, 14.08, 14.02 ppm.

Acknowledgements

The authors acknowledge the generous support from the National Science Centre: grant OPUS no. 2012/07/B/ST5/02016, ETIUDA 2014/12/T/ST5/00113, a Grant-in-Aid for Scientific Research (C) (no. 26410122) from the Japan Society for the Promotion of Science (JSPS) and a Grant-in-Aid for Scientific Research on Innovative Areas "Stimuli-responsive Chemical Species for Creation of Functional Molecules" (no. l5H00952) from the Ministry of Education, Culture, Sports, Science and Technology (MEXT) of Japan.

References

1 K. L. Brown, *Chem. Rev.*, 2005, **105**, 2075.
2 B. Kraütler, B. T. Golding and D. Arigoni, *Vitamin B_{12} and B_{12}-Proteins*, Wiley-VCH, 2008.
3 K. Gruber, B. Puffer and B. Kraütler, *Chem. Soc. Rev.*, 2011, **40**, 4346.
4 R. Banerjee, *Chemistry and Biochemistry of B_{12}*, John Wiley & Sons, 1999.
5 J. M. Pratt, *Chem. Soc. Rev.*, 1985, **14**, 161.
6 M. Giedyk, K. Goliszewska and D. Gryko, *Chem. Soc. Rev.*, 2015, **44**, 3391.

7 Y. Hisaeda, *J. Synth. Org. Chem., Jpn.*, 1996, **54**, 859.
8 Y. Hisaeda and H. Shimakoshi, in *Handbook of Porphyrin Science*, World Scientific Publishing Co., 2010.
9 R. Scheffold, S. Busato, E. Eichenberger, R. Härter, H. Su, O. Tinembart, L. Walder, C. Weymuth and Z.-D. Zhang, in *Organic Free Radicals SE - 93*, ed. H. Fischer and H. Heimgartner, Springer, Berlin, Heidelberg, 1988, p. 187.
10 I. A. Dereven'kov, D. S. Salnikov, R. Silaghi-Dumitrescu, S. V. Makarov and O. I. Koifman, *Coord. Chem. Rev.*, 2016, **309**, 68.
11 K. O. Proinsias, M. Giedyk, D. Gryko and K. Ó. Proinsias, *Chem. Soc. Rev.*, 2013, **42**, 6605.
12 Y. Murakami, Y. Hisaeda and A. Kajihara, *Bull. Chem. Soc. Jpn.*, 1983, **56**, 3642.
13 H. Shimakoshi and Y. Hisaeda, *Angew. Chem., Int. Ed.*, 2015, **54**, 15439.
14 J. Xu, H. Shimakoshi and Y. Hisaeda, *J. Organomet. Chem.*, 2014, **782**, 89.
15 H. Shimakoshi and Y. Hisaeda, *ChemPlusChem*, 2014, **79**, 1250.
16 W. Zhang, H. Shimakoshi, N. Houfuku, X.-M. Song and Y. Hisaeda, *Dalton Trans.*, 2014, **43**, 13972.
17 Y. Hisaeda, T. Nishioka, Y. Inoue, K. Asada and T. Hayashi, *Coord. Chem. Rev.*, 2000, **198**, 21.
18 M. Giedyk, S. N. Fedosov and D. Gryko, *Chem. Commun.*, 2014, **50**, 4674.
19 Y. Murakami, Y. Hisaeda, A. Kajihara and T. Ohno, *Bull. Chem. Soc. Jpn.*, 1984, **57**, 405.
20 Y. Murakami, Y. Hisaeda, T. Ozaki and Y. Matsuda, *Chem. Lett.*, 1988, 469.
21 H. Shimakoshi, M. Tokunaga and Y. Hisaeda, *Dalton Trans.*, 2004, 878.
22 D. Lexa, J. M. Savéant and J. Zickler, *J. Am. Chem. Soc.*, 1980, **102**, 2654.
23 D. Lexa and J. M. Savéant, *Acc. Chem. Res.*, 1983, **16**, 235.
24 C. Männel-Croisé and F. Zelder, *Inorg. Chem.*, 2009, **48**, 1272.
25 F. H. Zelder, *Inorg. Chem.*, 2008, **47**, 1264.
26 L. Werthemann, ETH Zurich, 1968.